

**KECK GEOLOGY CONSORTIUM
PROCEEDINGS OF THE TWENTY-THIRD
ANNUAL KECK RESEARCH SYMPOSIUM IN GEOLOGY
ISSN# 1528-7491**

April 2010

Andrew P. de Wet
Editor & Keck Director
Franklin & Marshall College

Keck Geology Consortium
Franklin & Marshall College
PO Box 3003, Lanc. Pa, 17604

Lara Heister
Symposium Convenor
ExxonMobil Corp.

Keck Geology Consortium Member Institutions:

Amherst College, Beloit College, Carleton College, Colgate University, The College of Wooster, The Colorado College
Franklin & Marshall College, Macalester College, Mt Holyoke College, Oberlin College, Pomona College, Smith College, Trinity University
Union College, Washington & Lee University, Wesleyan University, Whitman College, Williams College

2009-2010 PROJECTS

SE ALASKA - EXHUMATION OF THE COAST MOUNTAINS BATHOLITH DURING THE GREENHOUSE TO ICEHOUSE TRANSITION IN SOUTHEAST ALASKA: A MULTIDISCIPLINARY STUDY OF THE PALEOGENE KOOTZNAHOO FM.

Faculty: Cameron Davidson (Carleton College), Karl Wirth (Macalester College), Tim White (Penn State University)

Students: Lenny Ancuta, Jordan Epstein, Nathan Evenson, Samantha Falcon, Alexander Gonzalez, Tiffany Henderson, Conor McNally, Julia Nave, Maria Princen

COLORADO – INTERDISCIPLINARY STUDIES IN THE CRITICAL ZONE, BOULDER CREEK CATCHMENT, FRONT RANGE, COLORADO.

Faculty: David Dethier (Williams) Students: Elizabeth Dengler, Evan Riddle, James Trotta

WISCONSIN - THE GEOLOGY AND ECOHYDROLOGY OF SPRINGS IN THE DRIFTLESS AREA OF SOUTHWEST WISCONSIN.

Faculty: Sue Swanson (Beloit) and Maureen Muldoon (UW-Oshkosh)

Students: Hannah Doherty, Elizabeth Forbes, Ashley Krutko, Mary Liang, Ethan Mamer, Miles Reed

OREGON - SOURCE TO SINK – WEATHERING OF VOLCANIC ROCKS AND THEIR INFLUENCE ON SOIL AND WATER CHEMISTRY IN CENTRAL OREGON.

Faculty: Holli Frey (Union) and Kathryn Szramek (Drake U.)

Students: Livia Capaldi, Matthew Harward, Matthew Kissane, Ashley Melendez, Julia Schwarz, Lauren Werckenthien

MONGOLIA - PALEOZOIC PALEOENVIRONMENTAL RECONSTRUCTION OF THE GOBI-ALTAI TERRANE, MONGOLIA.

Faculty: Connie Soja (Colgate), Paul Myrow (Colorado College), Jeff Over (SUNY-Geneseo), Chuluun Minjin (Mongolian University of Science and Technology)

Students: Uyanga Bold, Bilguun Dalaibaatar, Timothy Gibson, Badral Khurelbaatar, Madelyn Mette, Sara Oser, Adam Pellegrini, Jennifer Peteya, Munkh-Od Purevtseren, Nadine Reitman, Nicholas Sullivan, Zoe Vulgaropulos

KENAI - THE GEOMORPHOLOGY AND DATING OF HOLOCENE HIGH-WATER LEVELS ON THE KENAI PENINSULA, ALASKA

Faculty: Greg Wiles (The College of Wooster), Tom Lowell, (U. Cincinnati), Ed Berg (Kenai National Wildlife Refuge, Soldotna AK)

Students: Alena Giesche, Jessa Moser, Terry Workman

SVALBARD - HOLOCENE AND MODERN CLIMATE CHANGE IN THE HIGH ARCTIC, SVALBARD, NORWAY.

Faculty: Al Werner (Mount Holyoke College), Steve Roof (Hampshire College), Mike Retelle (Bates College)

Students: Travis Brown, Chris Coleman, Franklin Dekker, Jacalyn Gorczynski, Alice Nelson, Alexander Nereson, David Vallencourt

UNALASKA - LATE CENOZOIC VOLCANISM IN THE ALEUTIAN ARC: EXAMINING THE PRE-HOLOCENE RECORD ON UNALASKA ISLAND, AK.

Faculty: Kirsten Nicolaysen (Whitman College) and Rick Hazlett (Pomona College)

Students: Adam Curry, Allison Goldberg, Lauren Idleman, Allan Lerner, Max Siegrist, Clare Tochilin

**Funding Provided by: Keck Geology Consortium Member Institutions and NSF (NSF-REU: 0648782)
and ExxonMobil**

**Keck Geology Consortium: Projects 2009-2010
Short Contributions – UNALASKA**

**LATE CENOZOIC VOLCANISM IN THE ALEUTIAN ARC: EXAMINING THE
PRE-HOLOCENE RECORD ON UNALASKA ISLAND**

Project Faculty: *KIRSTEN NICOLAYSEN*: Whitman College
RICHARD HAZLETT: Pomona College

**GEOCHEMICAL INVESTIGATION OF THE RED CINDER PEAK AREA OF
MAKUSHIN VOLCANO, UNALASKA, ALASKA**

ADAM CURRY: Pomona College
Research Advisors: Jade Star Lackey and Richard Hazlett

**PETROLOGIC AND VOLCANIC HISTORY OF POINT TEBENKOF
IGNIMBRITE, UNALASKA, ALASKA**

ALLISON R. GOLDBERG: Williams College
Research Advisor: Reinhard A. Wobus

**$^{40}\text{Ar}/^{39}\text{Ar}$ DATING OF LAVAS FROM MAKUSHIN VOLCANO, ALASKA:
EVIDENCE FOR XENOCRYST CONTAMINATION**

LAUREN M. IDLEMAN: Colgate University
Research Advisor: Martin S. Wong

**ERUPTION DYNAMICS OF THE 7.7 KA DRIFTWOOD PUMICE-FALL,
MAKUSHIN VOLCANO, ALASKA**

ALLAN H. LERNER: Amherst College
Research Advisor: Peter D. Crowley, Amherst College

**GEOCHEMICAL VARIATION IN PRE-CALDERA AND HOLOCENE LAVAS
FROM MAKUSHIN VOLCANO, UNALASKA ISLAND, ALASKA**

MAX T. SIEGRIST: Beloit College
Research Advisor: Jim Rougvie

**PALEOMAGNETIC EVIDENCE AND IMPLICATIONS FOR STRUCTURAL
BLOCK ROTATION ON UNALASKA ISLAND**

CLARE TOCHILIN: Whitman College

Research Advisors: Kirsten Nicolaysen and Robert Varga

Funding provided by: Keck Geology Consortium Member Institutions and NSF (NSF-REU: 0648782)

Keck Geology Consortium
Franklin & Marshall College
PO Box 3003, Lancaster Pa, 17603
Keckgeology.org

GEOCHEMICAL INVESTIGATION OF THE RED CINDER POINT AREA OF MAKUSHIN VOLCANO, UNALASKA, ALASKA

ADAM CURRY

Pomona College

Research Advisors: Jade Star Lackey and Richard Hazlett

INTRODUCTION

This project presents a geochemical analysis of Pleistocene volcanic deposits of the Red Cinder Peak area of Makushin Volcano, Unalaska Island, AK.

This analysis aims to understand the petrogenesis of the Point Tebenkof Ignimbrite (PTI) and several lava flows from the northeast flank of Makushin Volcano shown in Figure 1. Comparison of the ~42 m thick ignimbrite to younger Makushin caldera-forming events is significant from a hazards point of view because it constrains the conditions that have led to large, caldera-forming eruptions at Makushin in the past, exemplified by the PTI. Any future eruptions of similar magnitude could potentially threaten the residents of the nearby town of Unalaska (including Dutch Harbor) as well as disrupt air traffic downwind of the Aleutian Islands. Geologically, this project is significant because the Holocene eruptive history of Makushin Volcano and its satellite vents have been well characterized (Nye et al., 1986; McConnell et al., 1997; Roach, 1997; Bean, 1999; Begét et al., 2000), but the Pleistocene eruptive and petrogenetic history of Makushin is much less studied.

Makushin Volcano is a 2,036 m-high, historically active stratovolcano in the eastern Aleutian arc on Unalaska Island, AK, just west of the ocean-continent crustal boundary (Nicolaysen and Hazlett, this volume). The Holocene record contains evidence for two large, caldera-forming eruptions in addition to 17 historical eruptions (VEI 1-3), making it one of the more historically active volcanoes in the Aleutians (Bean, 1999; Begét et al., 2000). The Holocene tephra analyzed in Bean (1999) displayed spider diagram patterns suggesting similar evolution from similar parental magmas. Contrastingly, Nye et al. (1986) found evidence in a geochemical study of 160 Pleistocene-Holocene samples for magma

mixing, crystal-melt disequilibria, and successive, small batches of chemically distinct magmas entering a shallow magmatic system. When comparing late-Pleistocene to Holocene flank vent cumulates to cumulates in lavas derived from magma supplying the main Makushin massif, Roach (1997) found that flank vent lavas reflected more mafic, monogenetic magma chambers whereas the Makushin massif lavas reflect a more evolved chamber with chemical zoning, multiple reinjections, and many eruptive episodes. These differences in character between Holocene and Pleistocene Makushin call for a better understanding of the pre-Holocene eruptive history, the goal of this project.

METHODOLOGY

Red Cinder Peak and Pt. Tebenkof comprise the western wall of Driftwood Bay and Valley (Fig. 2 of Nicolaysen and Hazlett, this volume). Keck colleague Allie Goldberg and I collected ~ 40 samples from a stratigraphic sequence of 12 pre-Holocene lava flows and established field relations of these deposits (Fig. 1). At the bottom, the basal contact of the Point Tebenkof Ignimbrite, here named, was not visible due to beach cobbles. Lithic, vitric, scoria, and pumice samples were collected from various levels within the ignimbrite. Whole rock analyses were done at Washington State University according to the methods of Johnson et al. (1997) using a ThermoARL x-ray fluorescence spectrometer (XRF) and an HP4500+ inductively-coupled plasma-mass spectrometer (ICP-MS). Values of $\delta^{18}\text{O}$ for individual olivine and plagioclase crystals were measured at University of Oregon using laser fluorination (Valley et al., 1995). Pb isotope analysis was conducted at the University of British Columbia's Pacific Centre for Isotopic and Geochemical Research using a Nu

Plasma multi-collector inductively coupled plasma-mass spectrometer (MC-ICP-MS) according to the methods of Weis et al. (2006). Analytical precision at two standard deviations is as follows: XRF achieved ± 0.09 wt. % for all major elements, ± 2.3 ppm for all trace elements; ICP-MS achieved ± 1.07 ppm for all trace elements except Sr (± 10.8 ppm); $\delta^{18}\text{O}$ achieved ± 0.14 ‰; and Pb isotopes achieved ± 0.0046 . Error bars are left out of all figures except those with $\delta^{18}\text{O}$ based on symbol size relative to analytical precision.

RESULTS

STRATIGRAPHY

The feature herein called Red Cinder Peak is labeled on maps as Red Cinder Dome, implying that all flows are related to such a satellite dome. Peak is used here because the feature is not a volcanic extrusive dome but a point resulting from glacial erosion. The sampled flows in Figure 1 most likely originated from the main vent of Makushin or a buried satellite vent.

The stratigraphy of Red Cinder Peak is subdivided into four subsections, based on stratigraphic location (Fig. 1). Section 1 is the ignimbrite at the base of the exposure, and section 2 includes the four basaltic-andesitic flows directly overlying the PTI. Flow BCA is dated at 139 ka (see Idleman, this volume). Sections 3 and 4 are basaltic andesite and andesite lava flows whose stratigraphic relationships are obscured by lack of horizontal continuity. The top flow of Section 4, EAR, outcrops just below glacial till of the last glacial maximum.

The Pt. Tebenkof Ignimbrite is an andesitic, dominantly lapilli ignimbrite which is pumice-poor and scoria-rich. The PTI records many distinct eruptive phases, and the main phase marks the appearance of mingled scoria clasts in which a dark matrix surrounds lighter colored pumice. The ignimbrite is topped with an ~8 m section of co-ignimbrite ashfall grading from tan to brick red. A detailed description of the PTI can be found in Goldberg, this volume.

PETROGRAPHY

All lavas contain phenocrysts of dominantly plagioclase+ clinopyroxene \pm olivine \pm orthopyroxene. Sieve textures and zoning in plagioclase crystals are prominent in flows above the PTI, but very few sieve textures or zoning occur within the ignimbrite's phenocrysts. Sieving occurs either in the middle of the crystal on the edges, or throughout the crystal. Cumulophyres of different combinations of plagioclase, pyroxene, and occasionally olivine are prevalent in

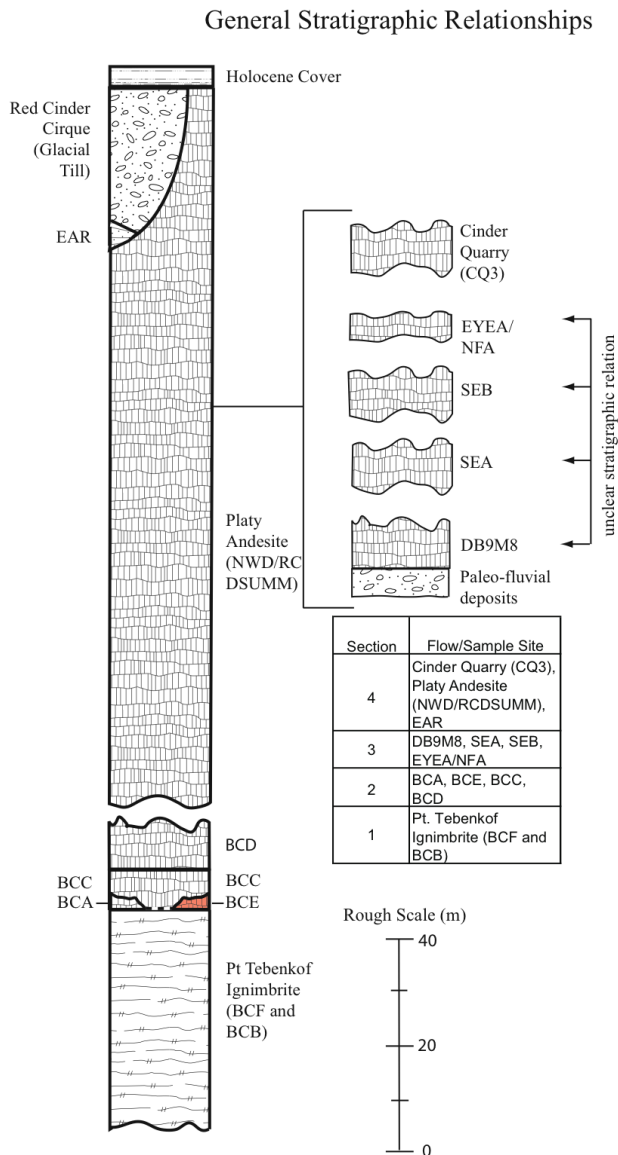


Figure 1. Stratigraphic relationships of Red Cinder Point area. The stratigraphic relationships are better exposed in Sections 1 and 2 compared to Sections 3 and 4.

the post-ignimbrite flows, while the ignimbrite has few cumuloxyres and crystals in general.

GEOCHEMISTRY

PTI samples (including lithic, vitric, scoria, and pumice samples from different layers) have normalized weight percent oxide abundances of SiO_2 (59.86-61.24), TiO_2 (0.97-1.114), Al_2O_3 (16.26-16.93), FeO^* (7-7.86), MgO (2.11-2.66), CaO (5.16-5.98), and K_2O (1.16-1.57). The PTI is a compositionally homogeneous ignimbrite up to the co-ignimbrite ash fall (not sampled). Subsequent flows have ranges of SiO_2 (49.66-63.72), TiO_2 (0.79-1.29), Al_2O_3 (15.11-18.87), FeO^* (6.11-10.19), MgO (1.73-8.99), CaO (4.31-11.89), and K_2O (0.63-2.21), normalized wt. %. These post-ignimbrite flows dis-

play much more heterogeneity than the ignimbrite. All samples except SEB and SEA fall into the tholeiitic geochemical field of Miyashiro (1974), which agrees with the previous geochemical analyses of Makushin (Nye et al., 1986; Bean, 1999).

Figure 2a-d shows trace element abundances of each stratigraphic section using the primitive mantle normalization of Sun and McDonough (1989) compared to the same author's NMORB values and average DSDP 183 (Plank and Langmuir, 1998). Nearly all samples from this study follow a typical island arc pattern, with BCC showing the only noticeable variation, including several dips below normal mid-ocean ridge basalt (NMORB) values. Figures 2e and 2f show the PTI compared to Holocene caldera-forming tephtras of Bean (1999) and mainly Holocene flank vent lavas of Roach (1997).

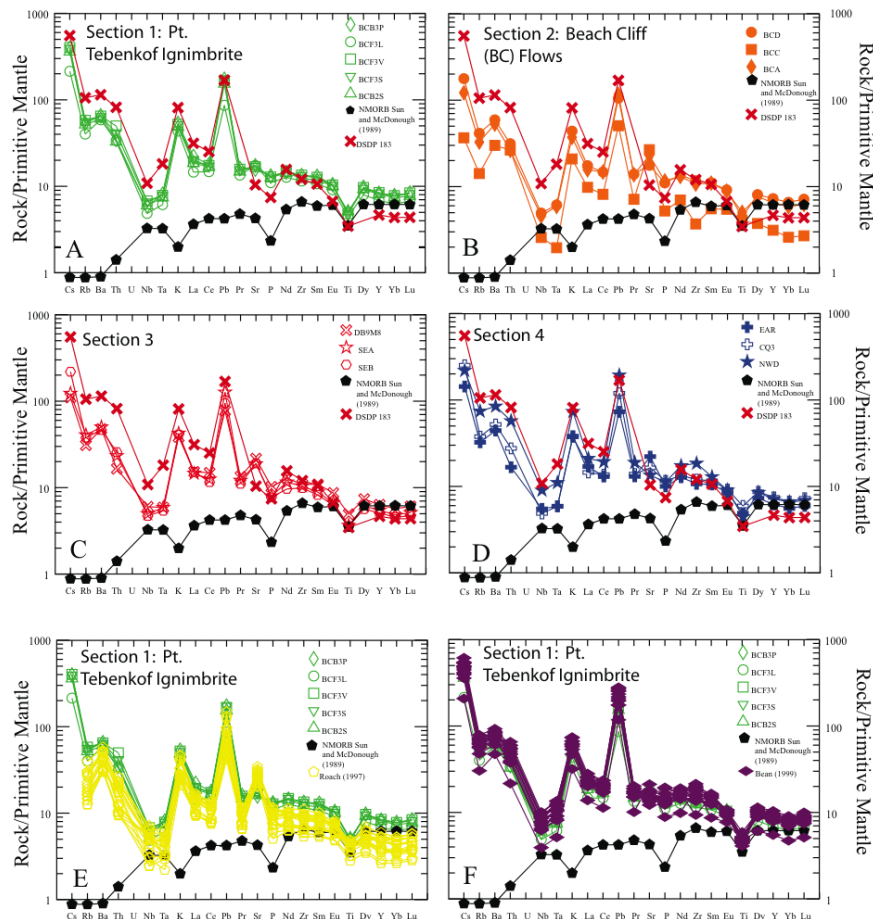


Figure 2. Primitive mantle-normalized spider diagrams showing samples in the present study compared to NMORB (Sun and McDonough, 1989), and DSDP 183 (Plank and Langmuir, 1998). Primitive mantle values are those of Sun and McDonough (1989). The homogeneity of the PTI is apparent in (a) whereas (b-d) show the greater variability of the subsequent lavas. Comparison of the PTI to (e) the mainly Holocene flank vent lavas of Roach (1997) and (f) Holocene caldera forming tephtras of Bean (1999) shows the Pleistocene ignimbrite is more fractionated relative to the Holocene lavas and slightly less fractionated relative to the Holocene tephtras, especially the two caldera forming events.

Figures 3 and 4 show the behavior of Th/La, Ba/La, Sm/La and $^{207}\text{Pb}/^{204}\text{Pb}$. Both Th/La and Ba/La are positively correlated to $^{207}\text{Pb}/^{204}\text{Pb}$, (Fig. 3a and 3b). In both instances the present samples plot between the MORB values and the DSDP 183 values. Furthermore, samples from this study plot between MORB and DSDP 183 values on a Th/La vs. Sm/La plot (Fig. 4).

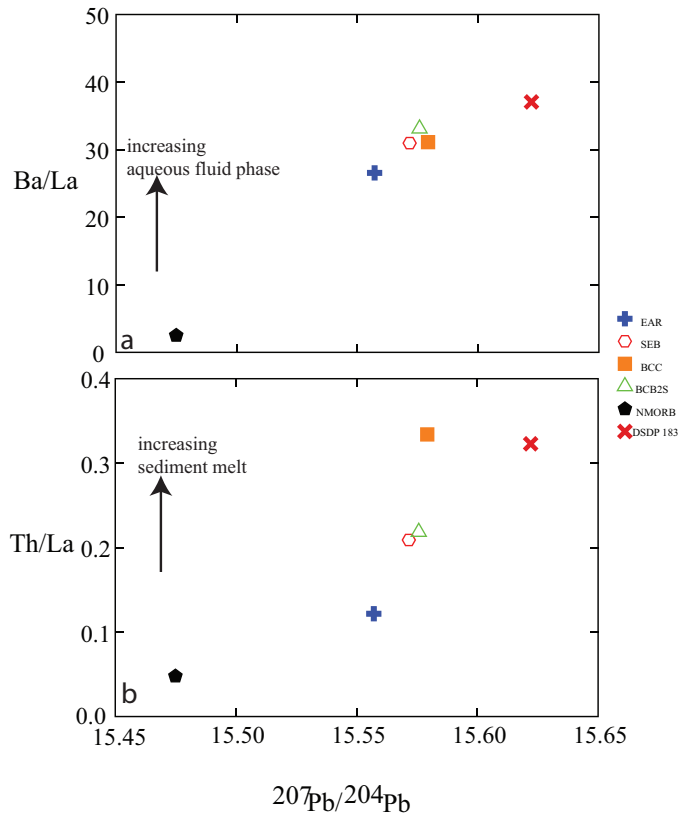


Figure 3. Ba/La, Th/La, and $^{207}\text{Pb}/^{204}\text{Pb}$ values for samples in the present study. Ba/La (aqueous phase proxy) and Th/La (sediment melt proxy) display positive correlation with $^{207}\text{Pb}/^{204}\text{Pb}$, and samples plot between NMORB (Sun and McDonough, 1989; Kelemen et al., 2003) and DSDP 183 (Plank and Langmuir, 1998; Kelemen et al., 2003). Error is smaller than the symbol size.

Olivine $\delta^{18}\text{O}$ values range from 4.32-5.48, and plagioclase $\delta^{18}\text{O}$ values range from 4.67-6.25 (Fig. 5a). Most samples plot below the arc mantle source value, and $\delta^{18}\text{O}$ values increase with stratigraphy. $\Delta^{18}\text{O}_{\text{OL-PLAG}}$ values plot above the magmatic equilibrium lines indicating disequilibrium between the minerals and the melt (Fig. 5b).

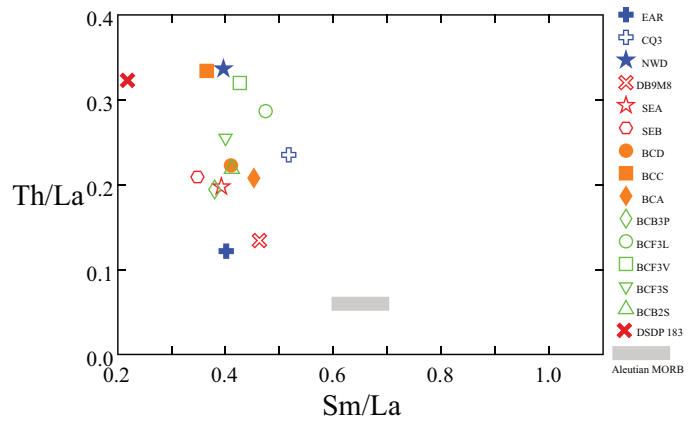


Figure 4. Th/La versus Sm/La plotted with Aleutian MORB (value taken from Plank, 2005) and DSDP values. The samples show an obvious mixing line between these end members. Error is smaller than the symbol size.

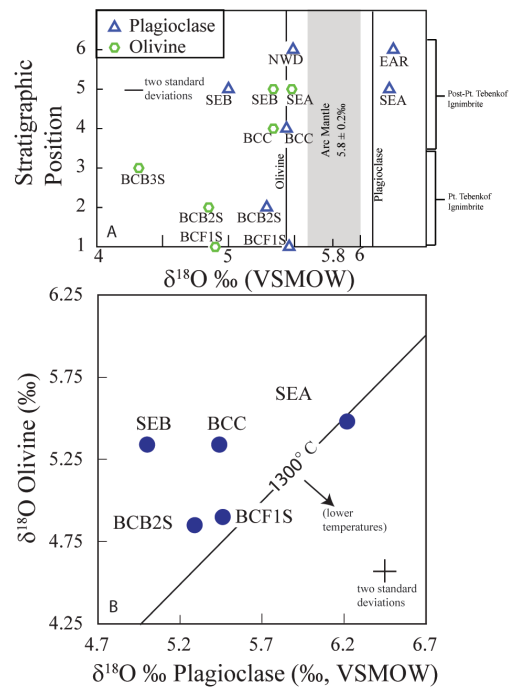


Figure 5. (A) $\delta^{18}\text{O}$ of individual plagioclase and olivine crystals plotted with arc mantle source value of Bindeman et al. (2004). (B) $\Delta^{18}\text{O}_{\text{OL-PLAG}}$ values plotted with lines of equilibrium at magmatic temperature 1300°C . Note the disequilibrium of all samples except SEA. Error is smaller than the symbol size.

DISCUSSION

The trace element patterns of these Pleistocene volcanics are typical of island arc settings (Fig. 2). The relative abundance of large ion lithophile elements (LILE) compared to high field strength

elements (HFSE) shows the influence of fluids in melt generation, as LILE are more fluid-mobile than HFSE. The similar values of HFSE of NMORB and my samples are best explained by a similar depleted mantle source. The only exception, flow BCC, has several HFSE values, Nb, Ta, Zr, Dy, Y, Yb, and Lu, lower than MORB, suggesting an even more depleted mantle source. That BCC in general has lower abundances than other samples implies its production by a higher degree of partial melting.

Figure 2e and 2f show that the PTI is enriched relative to the Roach (1997) Holocene flank vents, and only slightly depleted relative to the Bean (1999) Holocene caldera forming events. Because these trace element values track with SiO₂ abundance, the spider plot implies that the PTI reached a lower degree of fractionation of a similar parent magma compared to the Holocene caldera-forming eruptions prior to the catastrophic eruption of the PTI. That the samples in the present study are more akin to the samples of Bean (1997) than to Roach (1997) indicates that the PTI likely erupted from the main Makushin plumbing system rather than a satellite vent.

Kelemen et al. (2003) and Singer et al. (2007) discuss the positive correlation within the Aleutians of ²⁰⁷Pb/²⁰⁴Pb with sediment flux as well as Th/La and Ba/La. ²⁰⁷Pb/²⁰⁴Pb values increases to the east as does the calculated sediment flux (Kelemen et al., 2003; Singer et al., 2007). Th is high in marine sediments, low in the mantle, and relatively insoluble in fluids compared to Ba. Therefore, Th is used as a proxy for sediment melt, and Ba is used as a proxy for a fluid phase added to mantle peridotite melts. These flows show a wider range of Th/La than Ba/La, but the Ba/La values are closer overall to the DSDP 183 value (Fig. 3). This might suggest a consistent fluid release mechanism and a variable amount of sediment melting within the subduction zone. Figure 4, after Plank (2005), shows variable degrees of mixing between Pacific sediments and Aleutian MORB and helps explain the variation of the sample suite. BCC, NWD, and BCF3V are influenced most by subducted sediment, while EAR and DB9M8 are least sediment-influenced (Fig. 4).

The oxygen isotopes recorded in olivine and plagioclase crystals show a gradual increase of δ¹⁸O values going up stratigraphy (Fig. 3a). BCF-1S-1, BCB-2S, and BCB-3S (scoria from the first 3 layers of the ignimbrite, respectively) show the lowest olivine δ¹⁸O values, while SEA and SEB show the highest olivine δ¹⁸O values. Low δ¹⁸O phenocrysts can only be produced through magma that has somehow incorporated surface water, most likely through assimilation of hydrothermally altered crustal rocks (Bindeman et al., 2001). Δ¹⁸O_{OL-PLAG} values shown in Figure 5b show that plagioclase and olivine crystals in BCB-2S, BCF-1S-1, BCC, SEB, and SEA were not in equilibrium with the magma in which they grew. Because distribution coefficients dictate that plagioclase should have higher δ¹⁸O than olivine in a given magma, it is notable that SEB contains a plagioclase δ¹⁸O value lower than its olivine δ¹⁸O value. Figure 5 provides evidence for assimilation of hydrothermally altered crustal rocks, disequilibrium magma chambers, and possible magma mixing in sample SEB. This disequilibrium due to magma mixing is further supported by the prevalent sieve and zoning textures throughout the post-ignimbrite flows in addition to the magma mingling suggested by mottled scoria within the ignimbrite.

CONCLUSIONS

The volcanic rocks of Red Cinder Peak are derived from the main Makushin plumbing system rather than composing a satellite vent, and therefore the term Red Cinder Dome should not be used. Although most flows show similar trace element patterns (Fig. 2), much geochemical variability exists, especially regarding BCC. BCC seems to be more extensively melted from a more depleted source, but it also shows high Th/La ratios, indicating sediment melt. Most samples show some degree of sediment influence, but whether this is in the form of a sediment melt or aqueous fluids is to be determined. Given the similarities in spider diagrams, the cause of the PTI cannot be related to fundamental factors controlling such patterns, such as the mantle source or degree of partial melting. More likely, the PTI was caused by factors present in the petrography and

$\delta^{18}\text{O}$ values, specifically crustal assimilation of low- $\delta^{18}\text{O}$ rocks, disequilibrium between minerals and melt, and magma mixing.

ACKNOWLEDGEMENTS

In addition to those thanked in the general introduction to this project, I owe sincere thanks to Professors Jade Star Lackey, Kirsten Nicolaysen, and Rick Hazlett; Rick Conrey, Diane Johnson Cornelius, Laureen Wagoner, and Charles Knaack at WSU for their help on the XRF and ICP-MS machines; Professor Ilya Bindeman at the University of Oregon; and Bruno Kieffer and Dominique Weis of the Pacific Center for Isotopic and Geochemical Research.

REFERENCES

- Bean, K.W., 1999, The Holocene eruptive history and stratigraphy of Makushin Volcano, Unalaska Island, Alaska: Master of Science thesis, University of Alaska, Fairbanks.
- Begét, J.E., Nye, C.J., and Bean, K.W., 2000, Preliminary volcano-hazard assessment for Makushin Volcano, Alaska: Report of Investigations, Alaska Department of Natural Resources, Division of Geological and Geophysical Surveys, 22 p.
- Bindeman, I.N., Fournelle, J.H., and Valley, J.W., 2001, Low- $\delta^{18}\text{O}$ tephra from a compositionally zoned magma body: Fisher Caldera, Unimak Island, Aleutians: *Journal of Volcanology and Geothermal Research*, v. 111, 35-53.
- Bindeman, I.N., Ponomareva, V.V., Bailey, J.C., and Valley, J.W., 2004, Volcanic arc of Kamchatka: a province with high- $\delta^{18}\text{O}$ magma sources and large-scale $^{18}\text{O}/^{16}\text{O}$ depletion of the upper crust: *Geochimica et Cosmochimica Acta*, v. 68, no. 4, 841-865.
- Johnson, D. M., Hooper, P.R., and Conrey, R.M., 1997, XRF Analysis of Rocks and Minerals for Major and Trace Elements on a Single Low Dilution Li-tetraborate Fused Bead: *Advances in X-Ray Analysis*, v. 41, 843-867.
- Kelemen, P.B., Yogodzinski, G.M., Scholl, D.W., 2003, Along-Strike Variation in the Aleutian Island Arc: Genesis of High Mg Andesite and Implications for Continental Crust: *American Geophysical Union, Geophysical Monograph* 138, 223-276.
- Le Bas, M.J., Le Maitre, R.W., Streckeisen, A., and Zanettin, B., 1986, A Chemical Classification of Volcanic Rocks Based on the Total Alkali-Silica Diagram: *Journal of Petrology*, v. 27, 745-750.
- McConnell, V.S., Beget, J.E., Roach, A.L., Bean, K.W., and Nye, C.J., 1997, Geologic Map of the Makushin Volcanic Field, Unalaska Island, AK: USGS Alaska Volcano Observatory, Report of Investigations 97-20.
- Miyashiro, A., 1974, Volcanic Rock Series in Island Arcs and Active Continental Margins: *American Journal of Science*, v. 274, 321-355.
- Nye, C. J., Swanson, S. E., and Reeder, J. W., 1986, Petrology and Geochemistry of Quaternary Volcanic Rocks from Makushin Volcano, Central Aleutian Arc: Public Data File 86-80, Alaska Division of Geological and Geophysical Surveys, Fairbanks.
- Plank, T., 2005, Constraints from Thorium/Lanthanum on Sediment Recycling at Subduction Zones and the Evolution of the Continents: *Journal of Petrology*, v. 46, no. 5, 921-944.
- Plank, T. and Langmuir, C.H., 1998, The chemical composition of subducting sediment and its consequences for the crust and mantle: *Chemical Geology*, v. 154, 325-394.
- Roach, A.L., 1997, Crystal Clots in the Flank Vents and Lavas of the Makushin Volcanic Field: Implications for Cumulate Entrainment [Master's Thesis]: Fairbanks, University of Alaska, 126 p.
- Singer, B.S., Jicha, B.R., Leeman, W.P., Rogers, N.W.,

Thirwall, M.F., Ryan, J., Nicolaysen, K.E., 2007, Along-strike trace element and isotopic variation in Aleutian Island arc basalt: Subduction melts sediments and dehydrates serpentine: *Journal of Geophysical Research*, v. 112, 26 pp.

Sun, S and McDonough, W.F., 1989, Chemical and isotopic systematics of oceanic basalts: implications for mantle composition and processes: in Saunders, A.D. and Norry, M.J. (eds.), *Magma-tism in the Ocean Basins*, Geological Society of London Special Publication, no. 42, 313-345.

Valley, J. W., Kitchen, N., Kohn, M. J., Niendorf, C. R., and Spicuzza, M. J., 1995, UWG-2, a garnet standard for oxygen isotope ratios: Strategies for high precision and accuracy with laser heating: *Geochmica et Cosmochimica Acta*, v. 59, no. 24, 5223-5231.

Weis, D., Keiffer, B., Maerschalk, C., Barling, J., de Jong, J., Williams, G.A., Hanano, D., Pretorius, W., Mattielli, N., Scoates, J.S., Goolaerts, A., Friedman, R.M., Mahoney, J.B., 2006, High-precision isotopic characterization of USGS reference materials by TIMS and MC-ICP-MS: *Geochemistry Geophysics Geosystems*, v. 7, no. 8, 30 pp.